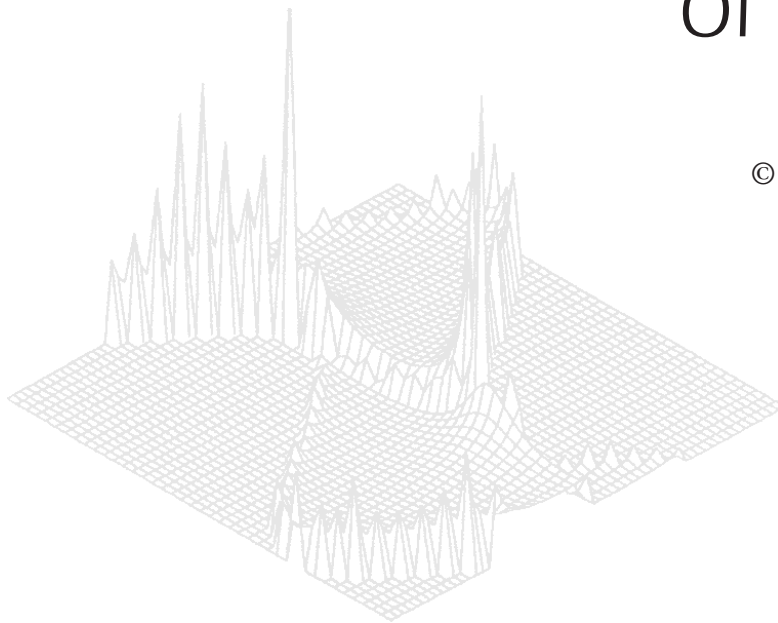

C S I R O P U B L I S H I N G

Australian Journal of Physics

Volume 52, 1999
© CSIRO Australia 1999



A journal for the publication of
original research in all branches of physics

www.publish.csiro.au/journals/ajp

All enquiries and manuscripts should be directed to

Australian Journal of Physics

CSIRO PUBLISHING

PO Box 1139 (150 Oxford St)

Collingwood

Vic. 3066

Australia

Telephone: 61 3 9662 7626

Facsimile: 61 3 9662 7611

Email: peter.robertson@publish.csiro.au



Published by **CSIRO PUBLISHING**
for CSIRO Australia and
the Australian Academy of Science



Calculation of the Exchange Constant in 2D Wigner Liquid*

V. V. Flambaum, I. V. Ponomarev and O. P. Sushkov

School of Physics, University of New South Wales,
Sydney, NSW 2052, Australia.
email: ilya@newt.phys.unsw.edu.au

Abstract

The recent observation of a two-dimensional (2D) metal–insulator transition in semiconductor devices and the strong influence of a magnetic field on the metallic phase has attracted a great deal of interest. This gives rise to the important theoretical question about the nature and the magnetic order of insulating and conducting phases. In the present paper we calculate (both analytically and numerically) the exchange constant for a two-dimensional Wigner liquid—the state with destroyed long-range order but preserved short-range order. It is demonstrated that there is an antiferromagnetic spin–spin interaction between nearest electrons. We also discuss a possible pairing of the electrons in a 2D Wigner crystal by the spin-Peierls mechanism.

It was shown long ago by Wigner (1934) that at sufficiently low density the electron gas (or electron fluid) of particles with $1/r$ repulsion undergoes a transition into a crystal state. This is because at low density the Coulomb interaction dominates over the kinetic energy and the correlated state becomes energetically favourable.

We consider a two-dimensional electron gas at zero temperature in the presence of a uniform neutralising background. Analysis of the lattice dynamics shows that the stable crystal structure in 2D is the triangular lattice (Bonsall and Maradudin 1977). The Wigner crystallisation has been observed for electrons at the surface of liquid helium (Grimes and Adams 1979). Another 2D system for which the electron density can be easily controlled is an inversion layer at a semiconductor surface (Chaplick 1971; for a review see Ando *et al.* 1982).

Theoretically, Wigner crystallisation has been studied using Monte Carlo simulations (Ceperley 1978; Tanatar and Ceperley 1989; Kwon *et al.* 1993). These calculations are quite reliable as far as the critical density is concerned. However, there is some controversy about a possible ferromagnetic Fermi liquid at a density slightly higher than the crystallisation density (Overhauser 1959, 1962; Rapisarda and Senatore 1996).

The interest in Wigner crystallisation has been renewed recently after observation of the insulator–conductor transition in dilute 2D electron systems (Kravchenko

* Refereed paper based on a contribution to the Eighth Gordon Godfrey Workshop on Condensed Matter Physics held at the University of New South Wales, Sydney, in November 1998.

et al. 1996). Although this transition probably takes place in the liquid phase, it is very close to the point of crystallisation. A very interesting feature of the transition is suppression of the conducting phase by the in-plane magnetic field (Simonian *et al.* 1997) which influences only the spin degrees of freedom. Therefore, the question about magnetic order (sign and magnitude of the exchange constant) is very important for understanding the nature of the transition.

In the present work we calculate the effective spin–spin interaction in a 2D Wigner crystal. This calculation is also valid for the Wigner liquid—the state with destroyed long-range order but preserved short-range order (Hansen and McDonald 1986).

To avoid misunderstanding let us note that our calculation does not show any magnetic phase transition in the liquid state (i.e. there is no ferromagnetic Fermi liquid between normal Fermi liquid and Wigner crystal). The state which we call a Wigner liquid is just a strongly renormalised normal Fermi liquid with an exponentially large effective carrier mass. We also keep in mind one of the well-known models of a liquid as a set of clusters of variable size with the same coordination number and symmetry as in the crystal. Nevertheless, magnetic properties of the Wigner liquid (and Wigner crystal) are quite unusual and somewhat similar to that of cuprate superconductors. There is a competition between superexchange (electron correlation) which gives an antiferromagnetic interaction between electron spins, and the usual exchange Coulomb interaction which gives a ferromagnetic contribution. The superexchange is proportional to t^2/U , where t is the parameter which describes hopping of an electron to a nearby site and U is the Coulomb repulsion for two electrons on the same site. As a result, both the superexchange and exchange are proportional to the squared overlap between the electron wave functions centred on the neighbouring sites of the Wigner crystal. Therefore, simple estimates cannot answer the question about the sign of the spin–spin interaction, and one needs to do more accurate calculations. To provide better understanding and reliability of the results we have performed these calculations in two ways, analytically and numerically.

The Hamiltonian of the system under consideration is

$$H = \sum_i \frac{\mathbf{p}_i^2}{2} + \sum_{i < j} \frac{1}{|\mathbf{r}_i - \mathbf{r}_j|} + \text{const}, \quad (1)$$

where \mathbf{p}_i and \mathbf{r}_i are 2D momentum and coordinate respectively. We use effective atomic units which means that all distances are measured in units of the effective Bohr radius $a_B^* = \hbar^2 \epsilon / m^* e^2$, and energies in units of $m^* e^4 / \hbar^2 \epsilon^2$. Here m^* is the effective electron mass, and ϵ is the dielectric constant which we assume to be independent of frequency. The number density of the electrons n is fixed by the condition of electroneutrality. An average distance r_s between the electrons is defined by $\pi r_s^2 = 1/n$. It is well established (Tanatar and Ceperley 1989) that the crystallisation to the triangular lattice occurs when $r_s \approx 37$. In the presence of ‘disorder’ further localisation of the electrons stabilises the Wigner crystal at higher densities, $r_s \approx 10$ (Eguiluz *et al.* 1983; Chui and Tanatar 1995). The distance between the nearest sites in the lattice is equal to $a = \sqrt{2\pi/\sqrt{3}} r_s \approx 1.90 r_s$.

The electrostatic potential acting on the electron near the equilibrium position in the lattice is

$$U_1(r) \approx \text{const} + \frac{\gamma r^2}{2 a^3}, \quad (2)$$

where $r \ll a$ is the deviation from the equilibrium position. To find γ let us freeze all other electrons in their equilibrium positions and calculate $U_1(r)$. Accounting for the six nearest sites gives $\gamma = 3$, and summation over the entire lattice gives

$$\gamma = 3 \sum_{n=1}^{\infty} \sum_{k=0}^{n-1} \frac{1}{(n^2 + k^2 - kn)^{\frac{3}{2}}} = 5.5171. \quad (3)$$

The ground state electron wave function in the potential (2) is

$$\psi(r) = \frac{1}{\sqrt{\pi c}} e^{-r^2/2c^2}, \quad c = \frac{a^{\frac{3}{4}}}{\gamma^{\frac{1}{4}}}. \quad (4)$$

In the above calculation we assume that the size of the wave function is much smaller than the lattice spacing, $c \ll a$, or $(a\gamma)^{\frac{1}{4}} \gg 1$. This parameter, in fact, corresponds to the inverse Lindemann ratio,

$$\frac{a}{\sqrt{\langle r^2 \rangle}} = \frac{a}{c} = (a\gamma)^{\frac{1}{4}}.$$

For the crystallisation point this parameter equals $(a\gamma)^{\frac{1}{4}} = 4.4$ and, therefore, the approximation is well justified in the crystal state. We stress that the parameter appears in the exponent and therefore 4.4 is a very large value. Moreover, the approximation is justified in the liquid phase as soon as $(a\gamma)^{\frac{1}{4}} \gg 1$. The point is that the sum in equation (3) is saturated by two or three coordination circles and it is independent of the presence or absence of the long-range order. For the conditions in the experiments by Kravchenko *et al.* (1996) this parameter equals $(a\gamma)^{\frac{1}{4}} = 3.1$.

To find the magnitude of the spin-spin interaction constant (the constant J which can be substituted into the Heisenberg Hamiltonian $J \sum_{\langle i,j \rangle} \vec{S}_i \vec{S}_j$), we have to solve a two-particle problem, freezing all the electrons except the nearest two, which are shown by crosses in Fig. 1.

The Hamiltonian of the problem is

$$\hat{H} = \frac{\mathbf{p}_1^2}{2} + \frac{\mathbf{p}_2^2}{2} + U(\mathbf{r}_1) + U(\mathbf{r}_2) + \frac{1}{|\mathbf{r}_1 - \mathbf{r}_2|}, \quad (5)$$

where $U(\mathbf{r})$ is the potential of all frozen electrons (dots in Fig. 1). The splitting between the ground states for total spin $S = 1$ and $S = 0$ gives us the constant J :

$$J = (E_g^{S=1} - E_g^{S=0}) \equiv (E_A - E_S), \quad (6)$$

$$\hat{H}\Psi_S = E_S\Psi_S, \quad (7)$$

$$\hat{H}\Psi_A = E_A\Psi_A. \quad (8)$$

Because of Fermi statistics the two-electron wave function is antisymmetric with respect to permutation. Therefore, the symmetric coordinate wave function corresponds to spin $S = 0$ and the antisymmetric one to $S = 1$.

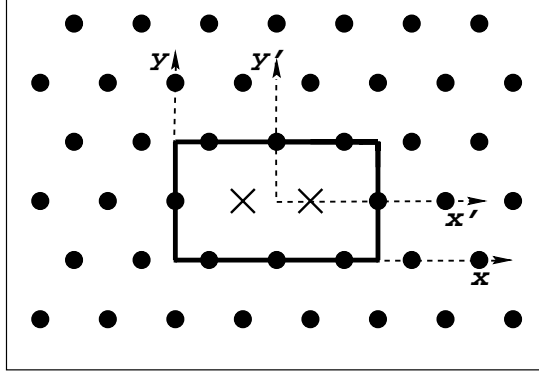


Fig. 1. Boundary conditions for the two-particle problem.

Of course the accurate solution of the problem can only be found (and has been found) numerically. However, to find the sign and the basic dependence J on a distance parameter a we performed an approximate analytical calculation. To this end, we follow the procedure, suggested long ago by Gor'kov and Pitaevskii for the calculation of the term splitting in hydrogen molecule (see Gor'kov and Pitaevskii 1964; Herring and Flicker 1964).

We multiply equation (7) by Ψ_A and (8) by Ψ_S , take the difference between the results and calculate the integral over some region in four-dimensional configuration space of the electrons. We choose the integration volume in which $x_1 \leq x_2$ [i.e. to the left of the hyperplane $\Sigma(x_1 = x_2)$]. Using the Hamiltonian (5) we obtain

$$(E_S - E_A) \iint_{\Omega} \Psi_A \Psi_S d\mathbf{r}_1 d\mathbf{r}_2 = \oint_{\Sigma} (\Psi_S \nabla \Psi_A - \Psi_A \nabla \Psi_S) d\Sigma. \quad (9)$$

The kinetic energy term on the right-hand side is reduced to the surface integral using

$$\Psi_S \nabla^2 \Psi_A - \Psi_A \nabla^2 \Psi_S = \nabla (\Psi_S \nabla \Psi_A - \Psi_A \nabla \Psi_S)$$

and an integration by parts.

Now we introduce combinations of the functions $\Psi_{1,2} = \sqrt{\frac{1}{2}}(\Psi_S \pm \Psi_A)$. They correspond to the states of 'distinguishable' particles when, for example for

$\Psi_1(\mathbf{r}_1, \mathbf{r}_2)$, the first electron is principally located near its equilibrium position $x = -a/2$ and the second electron near $x = a/2$. A simple calculation gives

$$\iint_{\Omega} \Psi_S \Psi_A d\mathbf{r}_1 d\mathbf{r}_2 = \frac{1}{2} \iint_{\Omega} (\Psi_1^2 - \Psi_2^2) d\mathbf{r}_1 d\mathbf{r}_2 \approx \frac{1}{2}.$$

Substituting the wave functions $\Psi_{1,2}$ into (9) and taking into account that under $\mathbf{r}_1 \leftrightarrow \mathbf{r}_2$ permutation the wave functions $\Psi_1 \leftrightarrow \Psi_2$, we obtain

$$J = -4 \int \left[\Psi_2 \frac{\partial \Psi_1}{\partial x_1} \right]_{x_1=x_2} dx_2 dy_1 dy_2. \quad (10)$$

The formula (10) shows that the main contribution to the exchange constant is given by the region where the electrons are close to each other. Indeed, the x coordinates of both electrons coincide ($x_1 = x_2$), however, the y coordinates may be different. In this case there are strong correlations between the positions of the electrons due to Coulomb repulsion. This means that we should go beyond the approximation where the two-particle wave function of the electrons is represented as a product of single-particles wave functions.

It is easy to take into account the effect of the correlations in the quadratic approximation. Assuming that the particles are distinguishable and oscillate near their equilibrium positions, we write the Hamiltonian in the following form:

$$\hat{H} = -\frac{\Delta_1}{2} - \frac{\Delta_2}{2} + \frac{\omega^2}{2} [(x_1 + a/2)^2 + y_1^2 + (x_2 - a/2)^2 + y_2^2] + \left\{ \frac{1}{|\mathbf{r}_1 - \mathbf{r}_2|} - \frac{1}{|\mathbf{r}_1 - \mathbf{a}/2|} - \frac{1}{|\mathbf{r}_2 + \mathbf{a}/2|} \right\}. \quad (11)$$

Here the frequency is $\omega = \sqrt{\gamma/a^3}$.

The Hamiltonian (11) is valid at small displacements x_i and y_i from their equilibrium positions. Expanding the last term in the curly brackets near $\tilde{x}_{1,2} = x_{1,2} \mp a/2$, we finally get the following Hamiltonian in the quadratic approximation:

$$\hat{H} = -\frac{\Delta_1}{2} - \frac{\Delta_2}{2} + \frac{\omega^2}{2} \left(\tilde{x}_1^2 + y_1^2 + \tilde{x}_2^2 + y_2^2 - \frac{4}{\gamma} \tilde{x}_1 \tilde{x}_2 + \frac{2}{\gamma} y_1 y_2 \right) + O(\tilde{x}^3/a^4). \quad (12)$$

Using an obvious change of variables

$$u, v = \frac{y_1 \pm y_2}{\sqrt{2}}, \quad \xi, \eta = \frac{x_1 \pm x_2}{\sqrt{2}}, \quad (13)$$

we separate the Hamiltonian (12) into four independent oscillators with frequencies $\omega_{u,v} = \sqrt{(\gamma \pm 1)/a^3}$ and $\omega_{\xi,\eta} = \sqrt{(\gamma \mp 2)/a^3}$. Thus, the ground state wave functions are

$$\Psi_1(u, v, \xi, \eta) = \frac{(\omega_u \omega_v \omega_\xi \omega_\eta)^{\frac{1}{4}}}{\pi} \exp\left(-\frac{1}{2}[\omega_u u^2 + \omega_v v^2 + \omega_\xi \xi^2 + \omega_\eta(\eta + a/\sqrt{2})^2]\right),$$

$$\Psi_2(u, v, \xi, \eta) = \Psi_1(u, v, \xi, -\eta). \quad (14)$$

Substituting equation (14) in (10) we obtain

$$J = +2\omega_\eta a \int [\Psi_2 \Psi_1]_{x_1=x_2} dx_2 dy_1 dy_2 = \sqrt{\frac{2}{\pi}} \omega_\eta^{\frac{3}{2}} a e^{-\omega_\eta a^2/2} \quad (15)$$

$$= (\gamma + 2)^{\frac{3}{4}} \sqrt{\frac{2}{\pi}} a^{-5/4} e^{-\sqrt{(\gamma+2)a}/2}. \quad (16)$$

This formula is presented in atomic units. In regular units it can be written as

$$J = + \frac{e^2}{\epsilon a} \left[\frac{a_B^*}{a} \frac{4(\gamma + 2)^3}{\pi^2} \right]^{\frac{1}{4}} \exp\left(-\sqrt{\frac{\gamma + 2}{4} \frac{a}{a_B^*}}\right)$$

$$= 3 \cdot 62 \frac{e^2}{\epsilon a} \left[\frac{a_B^*}{a} \right]^{\frac{1}{4}} \exp\left(-1 \cdot 37 \sqrt{\frac{a}{a_B^*}}\right). \quad (17)$$

The plus sign in the exchange constant shows that the system is antiferromagnetic. It is worth while noting that the exponent in (15) is different from $\exp(-\sqrt{\gamma a}/2)$, which appears if states $\Psi_{1,2}$ are represented by a product of independent single-particle wave functions (4).

In order to check the importance of correlations and find the correct exponent for J we have performed numerical calculations of the problem over a rectangle area (see Fig. 1). To be absolutely correct we have to impose periodic boundary conditions in the rectangle. However, the wave function is very small at the boundary and so the results are not sensitive to the boundary condition. It is much more convenient to make the wave function vanish at the boundary and this is the condition which we use in the present work.

The single particle basis set is given by (see Fig. 1)

$$\phi_i(\mathbf{r}) \equiv \phi_{nm}(x', y') = \frac{2}{\sqrt{AB}} \sin\left(\frac{\pi}{A} n x'\right) \sin\left(\frac{\pi}{B} m y'\right),$$

$$\varepsilon_i \equiv \varepsilon_{nm} = \frac{\pi^2}{2} \left[\frac{n^2}{A^2} + \frac{m^2}{B^2} \right], \quad (18)$$

where $A = 3a$ and $B = \sqrt{3}a$. Hence, for the two-electron problem the set is

$$|i\rangle \equiv |\mathbf{i}_1 \mathbf{i}_2\rangle = C_{\mathbf{i}_1 \mathbf{i}_2} [\phi_{\mathbf{i}_1}(\mathbf{r}_1) \phi_{\mathbf{i}_2}(\mathbf{r}_2) \pm \phi_{\mathbf{i}_1}(\mathbf{r}_2) \phi_{\mathbf{i}_2}(\mathbf{r}_1)], \quad E_i = \varepsilon_{\mathbf{i}_1} + \varepsilon_{\mathbf{i}_2}. \quad (19)$$

The + sign corresponds to $S = 0$ (antiferromagnetic) and the - sign to $S = 1$ (ferromagnetic). The normalisation coefficient is $C_{\mathbf{i}_1 \mathbf{i}_2} = \frac{1}{2}$ if $\mathbf{i}_1 = \mathbf{i}_2$; otherwise it equals $\sqrt{\frac{1}{2}}$. The matrix element of the Hamiltonian (5) is of the form

$$\langle i | \hat{H} | j \rangle = E_i \delta_{ij} + \langle i | V^{(1)} | j \rangle + \langle i | V^{(2)} | j \rangle, \quad (20)$$

where $\langle i | V^{(1,2)} | j \rangle$ are matrix elements of the single-particle potential and the two-particle interaction respectively:

$$\begin{aligned} \langle i | V^{(1)} | j \rangle &= 2 C_{\mathbf{i}_1 \mathbf{i}_2} C_{\mathbf{i}_3 \mathbf{i}_4} \left[V_{\mathbf{i}_1 \mathbf{i}_3}^{(1)} \delta_{\mathbf{i}_2 \mathbf{i}_4} \pm V_{\mathbf{i}_1 \mathbf{i}_4}^{(1)} \delta_{\mathbf{i}_2 \mathbf{i}_3} \pm V_{\mathbf{i}_2 \mathbf{i}_3}^{(1)} \delta_{\mathbf{i}_1 \mathbf{i}_4} + V_{\mathbf{i}_2 \mathbf{i}_4}^{(1)} \delta_{\mathbf{i}_1 \mathbf{i}_3} \right], \\ \langle i | V^{(2)} | j \rangle &= 2 C_{\mathbf{i}_1 \mathbf{i}_2} C_{\mathbf{i}_3 \mathbf{i}_4} [V_{i_1 i_2 i_3 i_4} \pm V_{i_1 i_2 i_4 i_3}]. \end{aligned} \quad (21)$$

To find J , which is exponentially small, we need a very large basis set. The most time consuming part is the computation of the two-particle matrix element $\langle i | V^{(2)} | j \rangle$, which formally is a four-dimensional integral. Fortunately, this integral can be reduced to one which is effectively one-dimensional. This reduction, which is given in the Appendix, allows us to perform computations with a Hilbert space size of up to $N = 1380$.

The numerical solution of the problem was performed for two different cases. Firstly, we considered all the frozen electrons (points at Fig. 1) as point-like charges, which means that the mean-field potential in this case is just the sum of the Coulomb potentials:

$$U(x, y) = \sum_{kl} u_0(|\mathbf{r}_{\mathbf{k}l} - \mathbf{r}|); \quad u_0(r) = 1/r. \quad (22)$$

The sum runs over sites of the triangular lattice.

Secondly, we considered the density of the frozen electrons to be distributed according to (4) and hence

$$U(x, y) = \sum_{kl} u_1(|\mathbf{r}_{\mathbf{k}l} - \mathbf{r}|); \quad u_1(r) = \frac{\sqrt{\pi}}{c} e^{-r^2/2c^2} I_0(r^2/2c^2), \quad (23)$$

where $I_0(x)$ is the modified Bessel function. In both cases all the results are very close and therefore we present plots only for the second case.

The matrices (20) for the ferromagnetic and antiferromagnetic cases were calculated and diagonalised. The Hilbert space was truncated at some high energy state. To be confident that the ground state was found with reasonable accuracy we used two basis sets with dimensions $N = 975$ and $N = 1380$, where N is the total number of two-particle states.

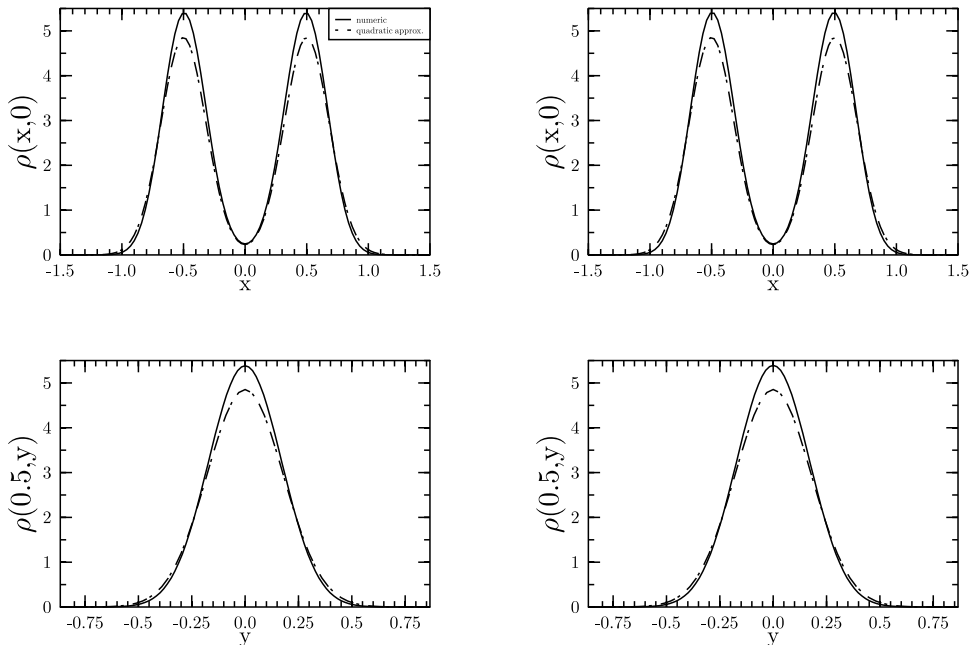


Fig. 2. Profiles of the density operator $\rho(\mathbf{r})$ for the antiferromagnetic (two upper plots) and ferromagnetic (lower plots) ground states for $a = 45$ ($r_s = 24$). The dot-dash curves show the analytical results in quadratic approximations (formula 25).

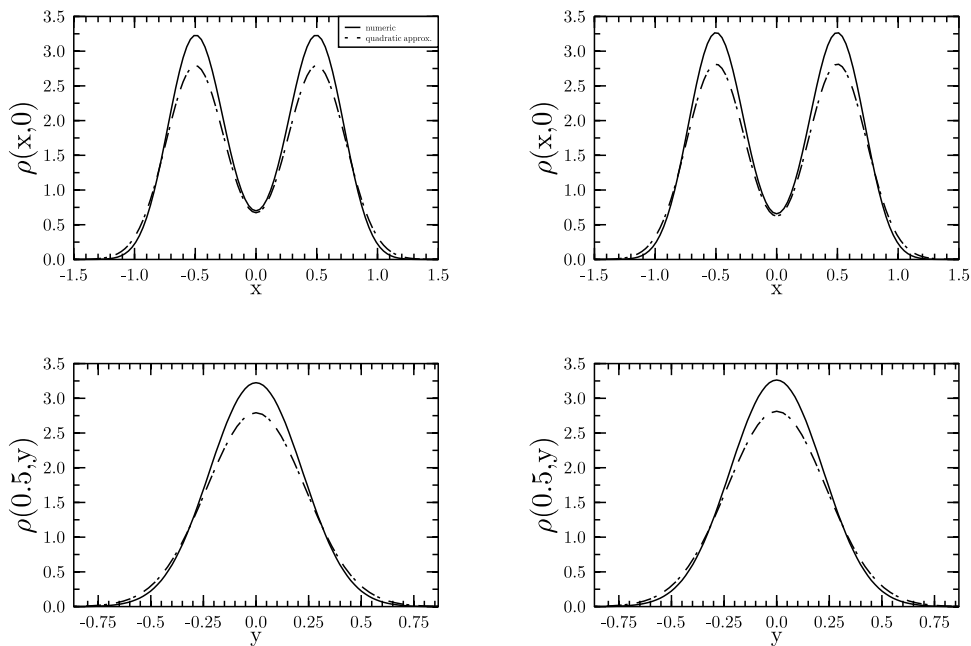


Fig. 3. Profiles of the density operator $\rho(\mathbf{r})$ for the antiferromagnetic (two upper plots) and ferromagnetic (lower plots) ground states for $a = 15$ ($r_s = 7.9$). The dot-dash curves show the analytical results in quadratic approximations (formula 25).

The plots of the ground-state electron density

$$\rho(\mathbf{r}) = \langle 0 | \delta(\mathbf{r} - \mathbf{r}_1) + \delta(\mathbf{r} - \mathbf{r}_2) | 0 \rangle \quad (24)$$

for $a = 45$, which corresponds to the limit of our calculations, are given in Fig. 2. Similar plots for $a = 15$, which corresponds to the conditions of the experiments by Kravchenko *et al.* (1996), are given in Fig. 3. The fact that the maxima coincide with the lattice sites tells us about the self-consistency of the method. The shape of the density operator near the equilibrium positions also corresponds to the expected Gaussian electron density, obtained from the combinations of the wave functions in (14):

$$\rho(x, y)_{S,A} = N_{S,A} \frac{2}{\pi} \sqrt{\frac{\omega_u \omega_v \omega_\xi \omega_\eta}{(\omega_u + \omega_v)(\omega_\xi + \omega_\eta)}} e^{-\tilde{\omega}_y y^2} \times \left[e^{-\tilde{\omega}_x (x+a/2)^2} + e^{-\tilde{\omega}_x (x-a/2)^2} \pm 2e^{-\omega_\eta a^2/2} e^{-\tilde{\omega}_x x^2} \right]. \quad (25)$$

Here $N_{S,A} = [1 \pm e^{-\omega_\eta a^2/2}]^{-1}$ is the normalisation coefficient due to the non-orthogonality of the functions Ψ_1 and Ψ_2 , while $\tilde{\omega}_y = 2\omega_u \omega_v / (\omega_u + \omega_v)$ and $\tilde{\omega}_x = 2\omega_\xi \omega_\eta / (\omega_\xi + \omega_\eta)$.

We found that for the whole region of the strength parameter a the antiferromagnetic ground state is always below the ferromagnetic one. We obtained the following values of the constant $J(a)$ for the parameters of the Kravchenko *et al.* experiments ($\epsilon = 8$, $m^* = 0.19m_e$):

$$J(15) = 6.66 \times 10^{-4} = 0.6 K, \quad J(45) = 1.48 \times 10^{-6} = 1.4 \times 10^{-3} K. \quad (26)$$

The experiments correspond to $a \simeq 15$. The behaviour of J , as expected, has an exponential dependence $\sim e^{-\delta\sqrt{a}}$. The plot of $\ln(J)$ versus \sqrt{a} in Fig. 4 summarises our results. Diamonds and crosses show the magnitude for different basis sets and nicely depict the truncation effects for large a and for a small number of basis states. The dot-dash line represents the theoretical curve (15) and the solid line is the best fit. We fitted our data by two different functions. For the first one we fixed the power of a in the pre-exponential factor [the analytical formula (15) gives $a^{-5/4}$]:

$$\ln(J) = C - \delta\sqrt{a} - \frac{5}{2} \ln(\sqrt{a})$$

and got $C = 2.25$ and $\delta = 1.595$.

In the second case we looked for the best parameters for

$$\ln(J) = C - \delta\sqrt{a} - \beta \ln(\sqrt{a}),$$

and we obtained $C = 2.02$, $\delta = 1.74$ and $\beta = 1.88$.

The analytical formula for J in equation (15) and more accurate fits of the numerical calculation data allows us to estimate the value of J for the Wigner crystal and Wigner liquid states in the region of large densities.

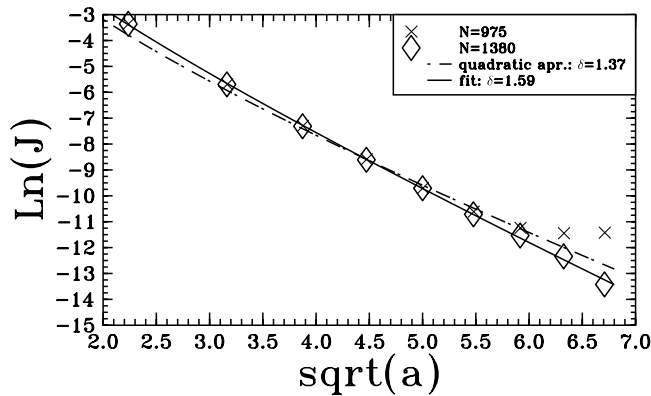


Fig. 4. Dependence of $\ln(J)$ on \sqrt{a} . Diamonds and crosses represent data for large ($N = 1380$) and shortened ($N = 975$) bases correspondingly. The dot-dash curve shows the theoretical curve of equation (15). The solid line is the best fit by $y = C - \delta\sqrt{a} - \beta\ln(a)$.

It is worth while stressing that the numerical computations were performed for the exact anisotropic crystalline potential, while our analytical solution (15) was obtained for the approximate quadratic Hamiltonian (12). The difference between the numerical and analytical exponential factors is

$$\delta_{\text{fit}} - \delta_{\text{an}} = 0.22 (\approx 14\%),$$

where $\delta_{\text{an}} = \sqrt{\gamma + 2}/2 = 1.37$. This difference comes from the higher order terms in the expansion of the Hamiltonian (11). Of course, our analytical method has a limited accuracy since, strictly speaking, there are no grounds for neglecting these terms [because the main contribution to the integral (15) is given by the region where $x/a \sim 1/2$]. Nevertheless, the very good agreement between the analytical and numerical results for the electron densities (Figs 2 and 3) and for the functional dependence $J(a)$ (Fig. 4) implies that our analytical treatment incorporates the main features of the problem. The recent numerical calculations of the exchange constant based on Monte Carlo simulations (Chakravarty *et al.* 1998) show good agreement with our result.

It would be instructive to discuss the difference between the exchange constant of the hydrogen molecule H_2 (Gor'kov and Pitaevskii 1964) and the Wigner crystal (or Wigner liquid). In the former case the exponent of the two-particle wave function is determined by the attraction of electrons to their nuclei (i.e. by the exponent of the wave function in the H atom). In this case the electron-electron interaction only has an effect on the factor before the exponential function in J , and not on the exponential itself. In the Wigner crystal case each electron makes a potential well for the other. Therefore, the exponent in the exchange constant is modified by the correlations.

Due to geometric frustration collinear long-range antiferromagnetic order is, strictly speaking, not possible on a triangular lattice. The possible solution in this case is a system spin wave function which in the zero approximation consists of spin zero pairs. The antiferromagnetic interaction increases when the distance between the electrons decreases. Therefore, there should be a tendency for nearby electrons coupled to spin zero pairs to move slightly toward each other. This phenomenon is usually called the 'spin-Peierls' mechanism. For a three-dimensional Wigner crystal the pairing mechanism was discussed by Mouloupoulos and Ashcroft (1993).

We can make a simple estimate of this effect in the two-dimensional case. For these purposes let us consider the following picture. The energy of the electron

pair when placed on the lattice sites is [i.e. in the minima of its potential wells (2) and where the distance between the electrons is a]

$$W(0) = -J(a, 0). \quad (27)$$

Here we have (see equation 15)

$$J(a, 0) \equiv J_0 = \sqrt{\frac{2}{\pi}} \omega_\eta^{\frac{3}{2}} a e^{-\omega_\eta a^2/2}. \quad (28)$$

If the distance between the electrons decreases by a small amount $2x$, the potential energy of each electron increases but the magnitude of the exchange constant becomes larger as well, since the single electron wave functions overlap more strongly:

$$J(a, 2x) = \sqrt{\frac{2}{\pi}} \omega_\eta^{\frac{3}{2}} (a - 2x) e^{-\omega_\eta (a-2x)^2/2}. \quad (29)$$

Thus, the energy of the pair is

$$W(x) = 2 \times \frac{\omega_\eta^2 x^2}{2} - J(a, 2x). \quad (30)$$

Introducing a relative displacement $u = x/a$ ($u \ll 1$), we rewrite (30) in the following form:

$$W(u) = \omega_\eta^2 a^2 u^2 - J_0 (1 - 2u) e^{2\omega_\eta (u-u^2)}. \quad (31)$$

Then the optimal magnitude of the displacement is given by the condition of the minimum of $W(u)$:

$$\frac{\partial W(u)}{\partial u} = 0 \implies u_{\min} \approx \frac{J_0}{\omega_\eta} \left[1 - \frac{1}{\omega_\eta a^2} \right] = \frac{J_0 \delta}{\omega_\eta}, \quad (32)$$

and the change in the energy is

$$\Delta W = W(u_{\min}) - W(0) = -J_0^2 a^2 \delta^2. \quad (33)$$

Thus, the reduction in energy is of second order in J_0 . It is a very small correction and in real systems this effect might be suppressed by other mechanisms. The parameters of the experiments (Kravchenko *et al.* 1996; Simonian *et al.* 1997) correspond to $u_{\min} = 1.5 \times 10^{-2}$ and $\Delta W \approx 10^{-4} = 8 \times 10^{-2}$ K.

However, the value of the spin-spin interaction constant itself in those experiments $J = J(15)$ is comparable with the energy μH . Here H is the critical magnetic field destroying conductivity. We can speculate that this field effectively transforms the system to a ferromagnetic state. In the ferromagnetic state the conductivity should be smaller than in the antiferromagnetic state. Indeed, in the antiferromagnetic state hopping of electrons with opposite spins from one site to another is allowed by the Pauli principle. The magnetic field rearranges spins in the same direction. In this case such hopping is suppressed by Pauli blocking. This possibly destroys the conductivity.

Acknowledgments

We are grateful to M. Kuchiev, L. Świerkowski, D. Neilson, D. Shepelyansky and G. Gribakin for useful discussions. V.V.F. is grateful to the Special Research Centre for the Subatomic Structure of Matter, University of Adelaide where part of this work has been done. This work is supported by the Australian Research Council.

References

- Ando, T., Fowler, A. B., and Stern, F. (1982). *Rev. Mod. Phys.* **54**, 437.
 Bonsall, L., and Maradudin, A. A. (1977). *Phys. Rev. B* **15**, 1959.
 Ceperley, D. M. (1978). *Phys. Rev. B* **18**, 3126.
 Chakravarty, S., Kivelson, S., Nayak, C., and Völker, K. (1998). Unpublished, cond-mat/9805383.
 Chaplick, A. V. (1971). *Sov. Phys. JETP* **35**, 395.
 Chui, S. T., and Tanatar, B. (1995). *Phys. Rev. Lett.* **74**, 458.
 Eguiluz, A. G., Maradudin, A. A., and Elliott, R. J. (1983). *Phys. Rev. B* **27**, 4933.
 Gor'kov, L. P., and Pitaevskii, L. P. (1964). *Sov. Phys. Doklady* **8**, 788.
 Grimes, C. C., and Adams, G. (1979). *Phys. Rev. Lett.* **42**, 795.
 Hansen, J. P., and McDonald, I. R. (1986). 'Theory of Simple Liquids' (Academic: New York).
 Herring, C., and Flicker, M. (1964). *Phys. Rev.* **134**, A362.
 Kravchenko, S. V., Simonian, D., Sarachik, M. P., Mason, W., and Furneaux, J. E. (1996). *Phys. Rev. Lett.* **77**, 4938.
 Kwon, Y., Ceperley, D. M., and Martin, R. M. (1993). *Phys. Rev. B* **48**, 12037.
 Mouloupoulos, K., and Ashcroft, N. W. (1993). *Phys. Rev. B* **48**, 11646.
 Overhauser, A. W. (1959). *Phys. Rev. Lett.* **3**, 414.
 Overhauser, A. W. (1962). *Phys. Rev.* **128**, 1437.
 Rapisarda, F., and Senatore, G. (1996). *Aust. J. Phys.* **49**, 161.
 Simonian, D., Kravchenko, S. V., Sarachik, M. P., and Pudalov, V. M. (1997). *Phys. Rev. Lett.* **79**, 2304.
 Tanatar, B., and Ceperley, D. M. (1989). *Phys. Rev. B* **39**, 5005.
 Wigner, E. (1934). *Phys. Rev.* **46**, 1002.

Appendix: Matrix Elements of the Interaction

The eigenfunctions and eigenvalues for the single-electron problem in the two-dimensional rectangle with sides $A = 3a$ and $B = \sqrt{3}a$ are given by equation (18). The matrix element of the Coulomb interaction between two unfrozen electrons is given by the integral over the rectangle's area

$$V_{i_1 i_2 i_3 i_4} = \int \phi_{i_3}(\mathbf{r}'_1)^* \phi_{i_4}(\mathbf{r}'_2)^* \frac{1}{|\mathbf{r}'_1 - \mathbf{r}'_2|} \phi_{i_1}(\mathbf{r}'_1) \phi_{i_2}(\mathbf{r}'_2) d^2 r'_1 d^2 r'_2. \quad (\text{A1})$$

It is convenient to change variables (see Fig. 1):

$$u = x'_1 - x'_2, \quad v = y'_1 - y'_2, \quad x''_2 = x'_2, \quad y''_2 = y'_2. \quad (\text{A2})$$

Introducing the notation $\tilde{u} = \pi u/A$, $\tilde{v} = \pi v/B$, and

$$F_{n_1 n_2 n_3 n_4}(\tilde{x}_1, \tilde{x}_2) = 4 \sin(\tilde{x}_1 n_1) \sin(\tilde{x}_1 n_3) \sin(\tilde{x}_2 n_2) \sin(\tilde{x}_2 n_4),$$

$$W_{n_1 n_2 n_3 n_4}(\tilde{u}) = \int_0^{\pi - \tilde{u}} F_{n_1 n_2 n_3 n_4}(\tilde{x}_2 + \tilde{u}, \tilde{x}_2) d\tilde{x}_2,$$

$$J_{n_1 n_2 n_3 n_4} = \frac{1}{2} [1 + (-1)^{n_1 + n_2 + n_3 + n_4}], \quad (\text{A3})$$

the matrix element (A1) can be rewritten as

$$V_{i_1 i_2 i_3 i_4} = J_{n_1 n_2 n_3 n_4} J_{m_1 m_2 m_3 m_4} \frac{4}{AB\pi^2} \times \int_0^A \int_0^B W_{n_1 n_2 n_3 n_4}(\tilde{u}) W_{m_1 m_2 m_3 m_4}(\tilde{v}) \frac{du dv}{\sqrt{u^2 + v^2}}. \quad (A4)$$

In this transformation we use the following relation:

$$\int_0^{\pi-\tilde{u}} F_{n_1 n_2 n_3 n_4}(x, x + \tilde{u}) dx = (-1)^{n_1+n_2+n_3+n_4} \int_0^{\pi-\tilde{u}} F_{n_1 n_2 n_3 n_4}(x + \tilde{u}, x) dx.$$

It is convenient to calculate the double integral (A4) using polar coordinates $\tilde{u} = \pi u/A = \sqrt{\frac{1}{3}}r \cos t$, $\tilde{v} = \pi v/B = r \sin t$. Taking into account that $\tan^{-1}(B/A) = \pi/6$ we find that

$$V_{i_1 i_2 i_3 i_4} = J_{n_1 n_2 n_3 n_4} J_{m_1 m_2 m_3 m_4} \frac{4}{3\pi^3} [V_1 + V_2]$$

$$V_1 = \int_0^{\pi/6} dt \int_0^{\pi\sqrt{3}/\cos t} W_{n_1 n_2 n_3 n_4}(\cos t/\sqrt{3}) W_{m_1 m_2 m_3 m_4}(r \sin t) dr,$$

$$V_2 = \int_0^{\pi/3} dt \int_0^{\pi/\cos t} W_{n_1 n_2 n_3 n_4}(r \sin t/\sqrt{3}) W_{m_1 m_2 m_3 m_4}(r \cos t) dr. \quad (A5)$$

In order to write down an analytical expression for the function $W_{n_1 n_2 n_3 n_4}(\tilde{u})$ let us introduce the following notation:

$$\begin{cases} n = |n_3 - n_1|, & n = 0, 1, 2, \dots \\ m = |n_4 - n_2|, & m = 0, 1, 2, \dots \\ l = n_3 + n_1, & l = 2, 3, \dots \\ k = n_4 + n_2, & k = 2, 3, \dots \end{cases}. \quad (A6)$$

Using (A3) one can find that

$$W_{n_1 n_2 n_3 n_4}(\tilde{u}) = \begin{cases} f_1(n, m, l, k; \tilde{u}) & \\ f_2(n, l, k; \tilde{u}) & \text{if } n = m \neq 0 \\ f_2(l, n, m; \tilde{u}) & \text{if } l = k \\ -f_2(n, m, l; \tilde{u}) & \text{if } n = k \\ -f_2(m, n, k; \tilde{u}) & \text{if } m = l \\ f_3(l, k; \tilde{u}) & \text{if } n = m = 0 \\ f_4(n, l; \tilde{u}) & \text{if } n = m \neq 0 \text{ and } l = k \\ f_5(l; \tilde{u}) & \text{if } n = m = 0 \text{ and } l = k, \end{cases} \quad (A7)$$

where

$$\begin{aligned}
 f_1(n, m, l, k; u) &= \frac{n \sin(nu) (k^2 - m^2)}{(n^2 - k^2) (n^2 - m^2)} + \frac{m \sin(um) (l^2 - n^2)}{(m^2 - l^2) (m^2 - n^2)} - \frac{l \sin(lu) (k^2 - m^2)}{(l^2 - m^2) (l^2 - k^2)}, \\
 &\quad - \frac{k \sin(uk) (l^2 - n^2)}{(-n^2 + k^2) (k^2 - l^2)}, \\
 f_2(n, m, l; u) &= \frac{\pi - u}{2} \cos(nu) + \frac{\sin(nu)}{2n} \left(1 + 2 \frac{n^4 - m^2 l^2}{(n^2 - m^2) (n^2 - l^2)} \right), \\
 &\quad + \frac{m \sin(um) (n^2 - l^2)}{(m^2 - l^2) (m^2 - n^2)} + \frac{l \sin(lu) (n^2 - m^2)}{(l^2 - n^2) (l^2 - m^2)}, \\
 f_3(n, m; u) &= \pi - u - \frac{\sin(um) n^2}{(m^2 - n^2) m} - \frac{\sin(nu) m^2}{(n^2 - m^2) n}, \\
 f_4(n, m; u) &= \frac{\pi - u}{2} [\cos(nu) + \cos(um)] + \frac{\sin(nu)}{2n} \frac{3n^2 + m^2}{n^2 - m^2} + \frac{\sin(um)}{2m} \frac{3m^2 + n^2}{m^2 - n^2}, \\
 f_5(n; u) &= \pi - u + \frac{\pi - u}{2} \cos(nu) + \frac{3}{2n} \sin(nu). \tag{A8}
 \end{aligned}$$

This completes the description of the calculation procedure for the two-electron Coulomb matrix element. The advantage is that each of the two integrals in (A5) requires numerical work equivalent only to the computation of a 1D integral.

Calculation of the single-particle matrix element of the external potential $U(\mathbf{r})$ is much simpler. It is convenient to use x and y instead of x' and y' (see Fig. 1). Then we get

$$\begin{aligned}
 V_{\mathbf{i}_1 \mathbf{i}_3}^{(1)} &\equiv V_{\{n_1 m_1, n_3 m_3\}}^{(1)} = \frac{4}{AB} (-1)^{(n+m/2)} J_{n_1 n_3} J_{m_1 m_3} \int_0^{A/2} \int_0^{B/2} U(x, y) \\
 &\quad \times \left\{ \cos\left(\frac{\pi}{A} nx\right) - (-1)^{n_2} \cos\left(\frac{\pi}{A} lx\right) \right\} \left\{ \cos\left(\frac{\pi}{B} my\right) \right. \\
 &\quad \left. - (-1)^{m_2} \cos\left(\frac{\pi}{B} ky\right) \right\} dx dy, \tag{A9}
 \end{aligned}$$

where

$$\begin{cases} n = |n_3 - n_1| \\ m = |m_3 - m_1| \\ l = n_3 + n_1 \\ k = m_3 + m_1. \end{cases}$$